Downloaded from jnm.snmjournals.org by Universitaetsbibliothek Bern on January 8, 2020. For personal use only.
Journal of Nuclear Medicine, published on September 20, 2019 as doi:10.2967/jnumed.119.233031

Cholecystokinin-2 Receptor Agonist ^{177}Lu-PP-F11N for Radionuclide Therapy of Medullary Thyroid Carcinoma - Results of the Lumed Phase 0a Study

Christof Rottenburger[1]*, Guillaume P. Nicolas[1,2]*, Lisa McDougall[1], Felix Kaul[1,2], Michal Cachovan[3], A. Hans Vija[4], Roger Schibli[5], Susanne Geistlich[6], Anne Schumann[7], Tilman Rau[8], Katharina Glatz[9], Martin Behe[6], Emanuel R. Christ[2,10], Damian Wild[1,2].

[1]Division of Nuclear Medicine, University Hospital Basel, Switzerland, [2]Center for Neuroendocrine and Endocrine Tumors, University Hospital Basel, Switzerland, [3]Siemens Healthcare GmbH, Forchheim, Germany, [4]Molecular Imaging, Siemens Medical Solutions USA, Inc., Hoffman Estates, IL, USA, [5]Department of Chemistry and Applied Biosciences, Institute of Pharmaceutical Sciences, ETH, Zurich, Switzerland. [6]Center for Radiopharmaceutical Sciences, Paul Scherrer Institute, Villigen, Switzerland, [7]3B Pharmaceuticals GmbH, Berlin, Germany; [8]Institute of Pathology, University of Bern, Switzerland, [9]Institute of Pathology, University Hospital Basel, Switzerland, [10]Division of Endocrinology, Diabetology and Metabolism, University Hospital Basel, Switzerland.

*Authors contributed equally

Corresponding Author

Damian Wild, Division of Nuclear Medicine, University Hospital Basel, Petersgraben 4, CH-4031 Basel, Switzerland. Phone +41 (0)61 3286683, Fax +41 (0)61 2654925. E-mail: damian.wild@usb.ch

source: https://doi.org/10.7892/boris.138052 | downloaded: 18.7.2024

Downloaded from jnm.snmjournals.org by Universitaetsbibliothek Bern on January 8, 2020. For personal use only.

First author

Christof Rottenburger, Division of Nuclear Medicine, University Hospital Basel, Petersgraben 4, CH-4031 Basel, Switzerland. Phone +41 (0)61 3286551, Fax +41 (0)61 2654354. E-Mail: christof.rottenburger@usb.ch

Short running title: ^{177}Lu-PP-F11N for Radionuclide Therapy

Downloaded from jnm.snmjournals.org by Universitaetsbibliothek Bern on January 8, 2020. For personal use only.

ABSTRACT

Treatment of patients with advanced medullary thyroid carcinoma (MTC) is still a challenge. For more than 2 decades it is known that cholecystokinine-2 receptor (CCK2R) is a promising target for the treatment of MTC with radiolabeled minigastrin analogues. Unfortunately, kidney toxicity precluded their therapeutic application so far. In 6 consecutive patients we evaluated with advanced 3D dosimetry whether improved minigastrin analogue ^{177}Lu-DOTA-$(DGlu)_6$-Ala-Tyr-Gly-Trp-Nle-Asp-PheNH$_2$ (^{177}Lu-PP-F11N) is a suitable agent for the treatment of MTC. **Methods:** Patients received two injections of about 1 GBq (~80 µg) ^{177}Lu-PP-F11N with and without a solution of succinylated gelatin (SG, a plasma expander used for nephroprotection) in a random cross-over sequence in order to evaluate biodistribution, pharmacokinetics as well as tumor- and organ dosimetry. Electrocardiogram, blood count and blood chemistry were measured up to 12 weeks after administration of ^{177}Lu-PP-F11N to assess safety. **Results:** In all patients ^{177}Lu-PP-F11N accumulation was visible in tumor tissue, stomach and kidneys. Altogether 13 tumors were eligible for dosimetry. The median (interquartile range = IQR) absorbed dose for tumors, stomach, kidneys and bone marrow was 0.88 Gy/GBq (0.85-1.04), 0.42 (0.25-1.01), 0.11 (0.07-0.13) and 0.028 (0.026-0.034). These resulted in a median (IQR) tumor-to-kidney dose ratio of 11.6 (8.11-14.4) without SG and 13.0 (10.2-18.6) with SG, which was not significantly different (P = 1.0). The median (IQR) tumor-to-stomach dose ratio was 3.34 (1.14-4.7). Adverse reactions (mainly hypotension, flushing and hypokalemia) were self-limiting and not higher than grade 1. **Conclusion:** ^{177}Lu-PP-F11N accumulates specifically in MTC at a dose that is sufficient for a therapeutic approach. With little kidney and bone marrow radiation dose ^{177}Lu-PP-F11N shows a promising biodistribution. The dose limiting organ is most likely the stomach. Further clinical studies are necessary to evaluate the maximum tolerated dose and the efficacy of ^{177}Lu-PP-F11N.

Key words: Cholecystokinine-2 receptor targeting, PRRT, ^{177}Lu-PP-FF11N, Theranostics

Downloaded from jnm.snmjournals.org by Universitaetsbibliothek Bern on January 8, 2020. For personal use only.

INTRODUCTION

According to recent data from the Surveillance, Epidemiology, and End Results database, medullary thyroid cancer (MTC) represents 1-2% of all thyroid cancers in the United States. Distant metastases can be detected clinically in 4-17% of patients at the time of diagnosis (*1,2*). MTC lacks accumulation of radioactive iodine and cytotoxic chemotherapy shows disappointing results for advanced MTC (*1*). The kinase inhibitors Vandetanib and Cabozantinib are approved for the treatment of MTC (*3,4*), but have not shown a significant effect on overall survival and may cause significant adverse reactions, including QT prolongation. Radionuclide therapy with compounds such as ^{90}Y-DOTATOC and Iodine-131 pretargeted anti-carcinoembryonic-antigen radioimmunotherapy were published in 2006/2007 with promising results (*5,6*). However, they were not introduced in clinical routine so far. Therefore, there is an unmet need for a more effective systemic therapy for patients with advanced MTC.

Specific targeting of MTC cells with radiolabeled minigastrin analogues has the potential to improve imaging and to allow peptide receptor radionuclide therapy, as >90% of MTC express the transmembrane G-protein coupled cholecystokinine-2 receptor (CCK2R) at a high density (*7*). Eight patients with advanced MTC were treated in a pilot study with the CCK2R specific yttrium-90 labeled minigastrin analogue ^{90}Y-DTPA-Glu$_1$-minigastrin (*8*). This resulted in partial remission in four and stable disease in two patients, lasting for up to 36 months. Unfortunately, nephrotoxicity and bone marrow toxicity limited the therapeutic application of this first radiolabeled minigastrin analogue.

Co-injection of nephroprotective substances is an often used approach to reduce nephrotoxicity. This was evaluated in rats and showed promising results with a 4% succinylated gelatin solution (SG, international marketing authorization as plasma expander: Gelofusine®, respectively Physiogel®). SG resulted in a 45% reduction of the renal cortex uptake of ^{111}In-DTPA-Glu$_1$-minigastrin (*9*), whereas the cationic amino acid lysine did not show a significant

Downloaded from jnm.snmjournals.org by Universitaetsbibliothek Bern on January 8, 2020. For personal use only.

effect. Another approach to reduce nephrotoxicity is to modify the compound itself: Amino acid chains with more than 5 glutamic acids in their sequence play an important role in the kidney re-uptake mechanism and may reduce kidney uptake (*10,11*). Such an approach was implemented by several groups and resulted in the development of a library of improved radiolabeled minigastrin analogues (*12-17*). Some of these new compounds show higher tumor uptake, higher tumor-to-kidney uptake ratios and higher serum stability, compared to the previously developed minigastrin analogues. One of the most promising new compounds is PP-F11N (DOTA-$(DGlu)_6$-Ala-Tyr-Gly-Trp-Nle-Asp-PheNH_2) which can be labeled with Lutetium-177, a widely used radionuclide that has not only excellent therapeutic properties but also a gamma ray component that allows acquisition of good quality images for a personalized treatment approach (theranostics), as well as dosimetry studies (*16*).

Here, we present the first-in-human results of ^{177}Lu-PP-F11N. Primary endpoint was the proof of CCK2R specific *in vivo* targeting and visualization of MTC metastases in correlation with histology, *in vitro* autoradiography or ^{18}F-DOPA PET/CT as standard of comparison. Secondary endpoints were safety, biodistribution, pharmacokinetics and radiation dosimetry after injection of a test dose of ^{177}Lu-PP-F11N with SG and without kidney protection in the same patient in a random cross-over order.

MATERIALS AND METHODS

Study Design and Patients

This is a prospective, randomized cross-over phase 0 single center study (clinicaltrials.gov: NCT02088645). The study was approved by the Institutional Review Board and all patients signed a written informed consent in accordance with the Declaration of Helsinki.

Downloaded from jnm.snmjournals.org by Universitaetsbibliothek Bern on January 8, 2020. For personal use only.

The main inclusion criteria were: histologically confirmed MTC with or without thyroidectomy and either elevated levels of calcitonin (> 100 pg/ml; respectively 29.2 pmol/l) and/or calcitonin-doubling time < 24 months. Patients who had received Vandetanib less than 3 weeks before the study and patients with reduced kidney or bone marrow function (calculated glomerular filtration rate < 60 ml/min / 1.73 m2 body surface, thrombocytes < 70'000/µl, leucocytes < 2'500/µl, hemoglobin < 8 g/dl) were not included.

Preparation of ^{177}Lu-PP-F11N

^{177}Lu-PP-F11N was produced according to good manufacturing practice by the Paul Scherrer Institute Villigen, Switzerland. The precursor peptide PP-F11N (2031.5 g/mol, GMP grade quality, piCHEM GmbH, Graz, Austria) is carrying a DOTA moiety on its N-terminal end, which allows stable chelation of Lutetium-177. GMP grade no carrier-added $^{177}LuCl_3$ (EndolucinBeta) was provided by ITG Isotope Technologies Garching GmbH, Garching, Germany. Radiolabeling of ^{177}Lu-PP-F11N was done in a synthesis module (PharmTracer by Eckert & Ziegler, Berlin, Germany). The reaction mixture, composed of 100 µg PP-F11N in aqueous 0.25 M ammonium-acetate buffer pH 5.5 (trace pure reagents, Sigma Aldrich, Buchs, Switzerland) and sodium ascorbate (USP grade) was incubated for 40 min at 60 °C with 1.7 GBq of EndolucinBeta. The reaction mixture was purified via C-18 SepPak column and sterile filtered into a bulk vial. The bulk product contained 20.9 mL 0.9 % saline, 1.25 mL ethanol, 1.75 mL water for injection, 0.1 ml DTPA (200 mg/mL), 250 mg sodium-ascorbate and ^{177}Lu-PP-F11N (total volume of 24 mL). After dispensing via a second sterile filter and taking aliquots for QC, the resulting product vial contained 20 ± 2 mL of final product tested for compliance with specifications (radiochemical purity: ≥ 95%; ^{177}Lu-DTPA: ≤ 2%; peptide content: < 100 µg of total PP-F11N; endotoxins: ≤ 175 EU). The product contained about 1 GBq of radioactivity at the end of shelf life, which is 24 h.

Downloaded from jnm.snmjournals.org by Universitaetsbibliothek Bern on January 8, 2020. For personal use only.

Injection

Patients received about 1 GBq ^{177}Lu-PP-F11N with and without SG in a random cross-over order within 4 weeks. Administration of SG (Physiogel®, B. Braun Medical AG, Sempach, Switzerland) was performed according to the IAEA, EANM, SNMMI guideline for PRRT (*18*), starting with a bolus dose of 6 ml/kg body weight/min 10 min before the start of the injection of ^{177}Lu-PP-F11N. After termination of ^{177}Lu-PP-F11N infusion, SG infusion was continued at a lower rate of 0.02 ml/kg body weight/min for 3 h.

Vital signs were recorded for 24 h and a 12-lead electrocardiogram was done before and 2 h after each injection. Clinical laboratory tests (hematology, biochemistry) were assessed until 12 weeks after the second injection. Adverse events were recorded and graded according to CTCAE 4.03.

Biodistribution, Pharmacokinetics and Dosimetry

Whole-body planar images and SPECT from neck to pelvis were performed on a calibrated SPECT/CT scanner (Symbia Intevo; Siemens Healthcare) at 1, 4, 24 and 72 h p.i. A combined SPECT/CT was acquired 24 h p.i. with a low-dose non-enhanced CT (130 kVp, 40 mA) for attenuation correction, anatomical reference and measurement of tumor diameters. The SPECT/CT scanner was equipped with a medium-energy, parallel-hole collimator and calibrated to a Selenium-75 source (Siemens Healthcare). Image acquisition was done with 2 detectors: 180° rotation per detector, 64 projections per detector, 20 s and 24 s (late scan at 72 h) per projection in a 128x128 matrix. The energy windows were set to 208 keV and 113 keV with a window width of 20 %. After data acquisition in list mode, a prototype version of xSPECT Quant (Siemens Healthcare) was used for Lutetium-177 quantification in order to get attenuation and scatter corrected quantitative datasets for 3D dosimetry studies.

Downloaded from jnm.snmjournals.org by Universitaetsbibliothek Bern on January 8, 2020. For personal use only.

Dosimetry of tumors, stomach and kidneys with and without co-administration of SG was performed with the Siemens Dosimetry Research Tool software version 5.4 (DRT, Siemens Medical Solutions, USA). DRT enables two methods for calculation of radiation dose: Voxel-based 3D dose kernel approach and a volume-based MIRD procedure, using quantitative SPECT/CT datasets with volumes of interest (VOIs) to create a time-activity fit (*19*). In our study the more established volume-based MIRD procedure was used.

^{177}Lu-PP-F11N positive tumors were identified on SPECT and correlated with the CT images. Afterwards, tumor VOIs were drawn based on CT volume. For kidney dosimetry, VOIs were defined on CT images by an automated segmentation algorithm. If necessary, contours were corrected manually, excluding the renal calices. Dosimetry of the stomach was hindered by stomach movement. To overcome this problem, a conservative measurement was chosen: a VOI of constant volume per patient (median 3.8 ml, range 1.9-25.6 ml) was placed over the stomach wall at the level of the maximum uptake across all time points in order to obtain residence time values (time-activity-fit) of the stomach wall. Residence time values of the stomach wall, kidneys and tumors were multiplied with S values (Monte Carlo simulations) and corrected for effective volumes. Tumor radiation doses were corrected for the partial volume effect, using recovery coefficients. Recovery coefficients were obtained by measurement of a NEMA NU 2007 phantom with a known activity concentration inside spheres of various diameters (smallest diameter was 10 mm which corresponds to a sphere of 0.52 cm^3). Recovery coefficients for tumor volumes lying between the measured sphere volumes were estimated by linear interpolation.

OLINDA/EXAM 1.0 software (Vanderbilt University, TN, USA) was used for the radiation dose calculation of the large intestine, bladder and the red bone marrow, see supplemental data. This is a 2D method based on planar images or blood sampling, using a blood-to-red-marrow activity

Downloaded from jnm.snmjournals.org by Universitaetsbibliothek Bern on January 8, 2020. For personal use only.

concentration ratio of 1, as recommended by the European Association of Nuclear Medicine (*20*).

Standard for Comparison

^{177}Lu-PP-F11N SPECT/CT scans were compared either with ^{18}F-DOPA (^{18}F-fluorodopa) PET/CT scans or histology, including *in vitro* autoradiography. ^{18}F-DOPA PET with contrast enhanced CT was performed 29-36 min after injection of 2.1-4.6 MBq/kg ^{18}F-DOPA according to the EANM guidelines (*21*) without carbidopa pretreatment in a time interval ranging from 7 months before until 3 months after performing the first ^{177}Lu-PP-F11N scan.

Fresh frozen tissue samples of one patient were available for *in vitro* autoradiography. *In vitro* CCK2R autoradiography was performed as described before (*7*). The sections were incubated with 6 x 10^5 cpm/ml of indium-111 labeled PP-F11N (45 MBq/nmol). In order to assess non-specific binding, an adjacent section of the same specimen was incubated in tracer solution containing additionally 200 nM of non-radioactive human gastrin (BACHEM, Bubendorf, Switzerland). The slides were then exposed to Biomax MR films (Carestream Health, Stuttgart, Germany) for 4 days. For signal quantification, a separate calibration curve, based on standard samples containing known amounts of radioactivity was recorded for each experiment. Subsequently, the autoradiograms were analyzed using MCID software (InterFocus, Linton, UK). For histopathological evaluation and localization of autoradiographic signal, adjacent slices were hematoxylin-eosin-stained.

Statistical Analysis

All variables were analyzed descriptively. Paired sign t-test, with a p-value <0.05 denoting statistical significance, was used to compare results obtained with and without SG (matched pairs).

Downloaded from jnm.snmjournals.org by Universitaetsbibliothek Bern on January 8, 2020. For personal use only.

RESULTS

Patients

Six consecutive patients with histologically proven MTC were screened and participated in the study. They all completed the study and were included in the proof of principle, safety, pharmacokinetic and dosimetry evaluation. All patients have had thyroidectomy previously. For further baseline demography and disease characteristics see Supplemental Table 1.

Proof of Principle

After infusion of 1040 ± 70 MBq (mean ± standard deviation; range: 915-1226 MBq) ^{177}Lu-PP-FF11N focal uptake concordant with pathological lesions was visible on whole body scintigraphy and SPECT/CT in all patients (Figs. 1 and 2). The median (IQR) volume of the tumors that underwent dosimetry was 0.72 cm^3 (range 0.57-1.51). Comparison with ^{18}F-DOPA PET/CT in 4 patients and with histology in 2 patients confirmed tumor specific ^{177}Lu-PP-F11N accumulation in all patients. Lesions identified with ^{177}Lu-PP-F11N SPECT/CT showed good correlation with ^{18}F-DOPA PET/CT, as 41 of 49 ^{18}F-DOPA positive lesions were ^{177}Lu-PP-F11N positive, too. On resected lesions from patient 3, *in vitro* autoradiography performed with ^{111}In-PP-F11N and histological assessment showed proof of tumor specific, CCK2R-mediated ^{177}Lu-PP-F11N accumulation in lymph node metastases (Fig. 3). One lymph node metastasis with a maximal diameter of 8 mm and 40% tumor involvement was not visible with SPECT/CT, but showed specific and intense ^{111}In-PP-FF11N uptake *in vitro* (Supplemental Fig. 1). The minimal size among detectable tumors with SPECT/CT was 8 mm, see Fig. 1.

Safety, Pharmacokinetics and Dosimetry

The short infusion (duration range: 4-6 minutes) of 79.3 ± 10.5 µg (mean ± SD, range: 67.0-94.5 µg) ^{177}Lu-PP-F11N was well tolerated with only grade 1 toxicity (Table 2).

Downloaded from jnm.snmjournals.org by Universitaetsbibliothek Bern on January 8, 2020. For personal use only.

Blood sampling of ^{177}Lu-PP-F11N revealed a bi-exponential blood clearance with an α half-life of 11 ± 3.3 min (with SG) versus 10.8 ± 5.4 min (without SG) and a β half-life of 162 ± 12 min versus 163 ± 14 min (mean ± SD); approximately 45% of the administered activity was cleared in the α phase. SG infusion starting 10 min before injection of ^{177}Lu-PP-FF11N did not significantly reduce renal absorbed dose: median (IQR) absorbed dose was 0.11 (0.07-0.13) Gy/GBq without SG and 0.06 (0.05-0.09) Gy/GBq with SG, p = 0.38 (two-sample paired sign test). The small amount of absorbed dose to the kidneys indicates low retention of ^{177}Lu-PP-F11N in the kidneys despite its predominant renal excretion (Fig. 2). The highest absorbed dose was determined for the tumors and stomach: median (IQR) absorbed dose without SG was 0.88 (0.85-1.04) Gy/GBq for tumors and 0.42 (0.25-1.01) Gy/GBq for the stomach, resulting in a median (IQR) tumor-to-stomach dose ratio of 3.34 (1.14-4.7), see Table 1. Blood sampling revealed a comparable median bone marrow dose with and without SG (0.032 and 0.028 Gy/GBq, respectively, Table 1). A summary of dosimetry results of all organs is given in Supplemental Table 2.

DISCUSSION

The main findings of this phase 0 clinical trial can be summarized as follows: 1) ^{177}Lu-PP-F11N shows specific accumulation with sufficiently high radiation dose in MTC tissue, potentially allowing a therapeutic approach; 2) *In vitro* data using autoradiography are consistent with *in vivo* data; 3) Acute toxicity of ^{177}Lu-PP-F11N is low; 4) dosimetry results suggest that the dose limiting organ is the stomach and 5) the co-administration of SG does not affect tumor-to-kidney dose ratio.

Even though the injected activity was low (1 GBq), ^{177}Lu-PP-F11N SPECT/CT imaging detected lesions in all patients. Forty-one of 49 ^{18}F-DOPA PET/CT positive lesions could also be identified with SPECT-imaging, with the smallest detected metastasis measuring only 8 mm,

Downloaded from jnm.snmjournals.org by Universitaetsbibliothek Bern on January 8, 2020. For personal use only.

confirming effective CCK2R targeting and low background activity with ^{177}Lu-PP-F11N. In one ^{177}Lu-PP-F11N SPECT negative lesion, *in vitro* autoradiography showed ^{111}In-PP-F11N specific accumulation in an 8 mm lymph node metastasis with 40% tumor infiltration. This example shows that even small SPECT negative metastases could potentially be treated with ^{177}Lu-PP-F11N. The tumor radiation doses calculated in our study are lower than those normally calculated for radionuclide therapy with Lutetium-177 labelled somatostatin-receptor subtype 2 (SSTR2) specific ligands in patients with non-MTC neuroendocrine tumors. For example, the median tumor dose for ^{177}Lu-PP-F11N in our study is 0.88 Gy/GBq versus 2.0 Gy/GBq for ^{177}Lu-DOTATATE in neuroendocrine tumors (*22*). On the other hand, *in vitro* autoradiography studies have shown a higher incidence of CCK2R than SST2R expression in MTC: iodine-125 labeled CCK2R agonist showed specific binding in >90% of MTC versus <30% with iodine-125 labeled SST2R agonist (*7,23*). Furthermore, radiation doses to organs such as kidneys and bone marrow were at least 3 times less with ^{177}Lu-PP-F11N than with ^{177}Lu-DOTATATE (*22*). Based on our dosimetry study, fractionated treatment with a cumulative activity of 50 GBq ^{177}Lu-PP-F11N should be possible without surpassing the maximal tolerated dose to the stomach, which is estimated to be 50 Gy based on external beam radiotherapy studies (*24*). Indeed, the 3rd quartile of the ^{177}Lu-PP-F11N absorbed dose to the stomach was 1 Gy/GBq. A cumulative activity of 50 GBq could potentially result in a mean absorbed tumor dose of 50 x 0.9 Gy (~45 Gy) or 50 x 3.6 Gy (~180 Gy) for patient 2, who showed the highest tumor absorbed dose.

Acute toxicity after injection of 67.0-94.5 µg ^{177}Lu-PP-F11N was low and within the range of adverse reactions known from the CCK2R agonist pentagastrine (calcitonin stimulation test) or other minigastrin analogues (*8*). Radiation induced toxicity was not observed after a cumulated activity of ~2 GBq ^{177}Lu-PP-F11N.

Calculated kidney radiation doses were low and resulted in higher median tumor-to-kidney radiation dose ratios, compared to the commonly used therapeutic radiotracer ^{177}Lu-DOTATATE

Downloaded from jnm.snmjournals.org by Universitaetsbibliothek Bern on January 8, 2020. For personal use only.

(11.6 versus 1.6) (*22*). In contrast to DTPA-Glu_1-minigastrin (*9*), the co-administration of SG did not significantly reduce the tumor-to-kidney dose ratio in our study. Therefore, nephroprotection with SG in combination with ^{177}Lu-PP-F11N is not beneficial and can be omitted, as kidney doses are already low. The stomach received the highest calculated organ radiation dose and is therefore most likely the dose limiting organ. This has been reported for CCK2R ligands before (*8*) and can be explained by specific binding of ^{177}Lu-PP-F11N to the CCK2R on neuroendocrine cells in the gastric mucosa, mainly enterochromaffine-like cells (*25*). Interestingly, stomach radiation doses in our patients were heterogeneous (0.18 - 2.07 Gy/GBq). The patient with the highest stomach dose (patient 5) had history of medication with proton pump inhibitors. The patient with the lowest dose (patient 4) received enteral tube feeding formula. Therefore, it can be speculated that gastric acidity and activity (digestion) might have a relevant effect on the stomach uptake. This would be in line with reported increase of enterochromaffine-like cells density and the thickness of gastric mucosa after chronic acid suppression by proton pump inhibitors (*25*). Radiation doses of the remaining organs, including bone marrow, were low and therefore they were not considered as risk organs for a therapeutic approach.

The evaluation of the different radiolabeled minigastrin derivatives differing in both, the C-terminal peptide binding moiety and the structural characteristics of the linker, revealed that the compounds with six D-glutamic acid residues within the amino acid chain belong to the most promising substances with an reasonable balance of tumor uptake and decreased kidney reabsorption (*11,12,16*). The pronounced hydrophilicity of such compounds is most likely the reason for the fast renal excretion and shorter blood half-life of ^{177}Lu-PP-F11N in comparison to ^{177}Lu-DOTATATE (β half-life of 163 ± 14 min versus 468 ± 150 min (mean ± SD)) (*22*), resulting in a lower tumor radiation dose. Future strategies to achieve higher tumor doses should be investigated and might consist in either increasing tumor uptake (e.g. by upregulation of CCK2R density selectively in MTC) or decreasing stomach uptake (e.g. via a specific diet or by manipulation of gastric acidity).

Downloaded from jnm.snmjournals.org by Universitaetsbibliothek Bern on January 8, 2020. For personal use only.

The main limitation of our study is the low number of evaluated subjects. This might affect the statistical significance of kidney dosimetry with and without SG. But even if SG has a significant nephroprotective effect, it appears unnecessary to expose patients to potentially severe SG-related toxicity (i.e. anaphylactic reactions), as ^{177}Lu-PP-FF11N shows per se low kidney uptake.

CONCLUSION

^{177}Lu-PP-F11N accumulates specifically in MTC lesions, resulting in a radiation dose level that is potentially sufficient for a therapeutic approach. The biodistribution of ^{177}Lu-PP-F11N appears to be favorable, with low kidney and bone marrow radiation dose. The dose limiting organ is most likely the stomach. Further clinical studies are necessary to evaluate the maximum tolerated dose and efficacy of ^{177}Lu-PP-F11N in MTC and other CCK2R expressing tumors. In doing so, the following clinical scenarios should be considered: postoperative adjuvant approach in high risk patients and palliative treatment of advanced, metastatic disease.

DISCLOSURES

Martin Béhé and Roger Schibli are inventors of patent application WO 2015/067473, which contents PP-F11N. Patent holder is Paul Scherrer Institute and the patent is licensed to Debiopharm International SA (Lausanne, Switzerland). ITG AG (Munich, Germany) supported the study with free $^{177}LuCl_3$ (EndolucinBeta®). The study was supported by the Swiss cancer research foundation (KFS-3170-02-2013), and the Nora van Meeuwen-Haefliger Stiftung, Basel. No other conflict of interest relevant to this article was reported.

Downloaded from jnm.snmjournals.org by Universitaetsbibliothek Bern on January 8, 2020. For personal use only.

ACKNOWLEDGMENTS

We thank Stefan Landolt and Marc Tautschnig from Paul Scherrer Institute, Isotope Technologies Garching for providing Lutetium-177 and Virginie Wersinger for excellent assistance.

KEY POINTS

QUESTION: Is it possible to target medullary thyroid carcinoma (MTC) lesions with ^{177}Lu-PP-F11N in humans?

PERTINENT FINDINGS: In a monocentric phase 0 proof of principle study, ^{177}Lu-PP-F11N shows low toxicity and specific accumulation in MTC tissue accumulation in all 6 included patients.

IMPLICATIONS FOR PATIENT CARE: ^{177}Lu-PP-F11N is a promising and safe radiopharmaceutical for peptide receptor radiotherapy of MTC.

Downloaded from jnm.snmjournals.org by Universitaetsbibliothek Bern on January 8, 2020. For personal use only.

REFERENCES

1. Wells SA Jr, Asa SL, Dralle H, et al. Revised American Thyroid Association guidelines for the management of medullary thyroid carcinoma. *Thyroid*. 2015;25:567-610.
2. Hadoux J, Pacini F, Tuttle RM, et al. Management of advanced medullary thyroid cancer. *Lancet Diabetes Endocrinol*. 2016;4:64-71.
3. Wells SA Jr, Robinson BG, Gagel RF, et al. Vandetanib in patients with locally advanced or metastatic medullary thyroid cancer: a randomized, double-blind phase III trial. *J Clin Oncol*. 2012:30:134-141.
4. Elisei R, Schlumberger MJ, Müller SP, et al. Cabozantinib in progressive medullary thyroid cancer. *J Clin Oncol*. 2013;31:3639-3646.
5. Iten F, Muller B, Schindler C, et al. Response to [90Yttrium-DOTA]-TOC treatment is associated with long-term survival benefit in metastasized medullary thyroid cancer: a phase II clinical trial. *Clin Cancer Res*. 2007;13:6696–6702.
6. Chatal JF, Campion L, Kraeber-Bodere F, et al. Survival improvement in patients with medullary thyroid carcinoma who undergo pretargeted anti-carcinoembryonic-antigen radioimmunotherapy: a collaborative study with the French Endocrine Tumor Group. *J Clin Oncol.* 2006;24:1705–1711.
7. Reubi JC, Schaer JC, Waser B. Cholecystokinin(CCK)-A and CCK-B/gastrin receptors in human tumors. *Cancer Res*. 1997;57:1377-1386.
8. Behr TM, Béhé MP. Cholecystokinin-B/Gastrin receptor-targeting peptides for staging and therapy of medullary thyroid cancer and other cholecystokinin-B receptor-expressing malignancies. *Semin Nucl Med*. 2002;32:97-109.
9. Gotthardt M, van Eerd-Vismale J, Oyen WJ, et al. Indication for different mechanisms of kidney uptake of radiolabeled peptides. *J Nucl Med*. 2007;48:596-601.
10. Béhé M, Kluge G, Becker W, et al. Use of polyglutamic acids to reduce uptake of radiometal-labeled minigastrin in the kidneys. *J Nucl Med*. 2005;46:1012-1015.

Downloaded from jnm.snmjournals.org by Universitaetsbibliothek Bern on January 8, 2020. For personal use only.

11. Ritler A, Shoshan MS, Deupi X, et al. Elucidating the structure-activity relationship of the pentaglutamic acid sequence of minigastrin with cholecystokinin receptor subtype 2. *Bioconjug Chem*. 2019;30:657-666.
12. Laverman P, Joosten L, Eek A, et al. Comparative biodistribution of 12 ^{111}In-labelled gastrin/CCK2 receptor-targeting peptides. *Eur J Nucl Med Mol Imaging*. 2011;38:1410-1416.
13. Kolenc-Peitl P, Mansi R, Tamma M, et al. Highly improved metabolic stability and pharmacokinetics of indium-111-DOTA-gastrin conjugates for targeting of the gastrin receptor. *J Med Chem*. 2011;54:2602-2609.
14. Ocak M, Helbok A, Rangger C, et al. Comparison of biological stability and metabolism of CCK2 receptor targeting peptides, a collaborative project under COST BM0607. *Eur J Nucl Med Mol Imaging*. 2011;38:1426-1435.
15. Fani M, Maecke HR. Radiopharmaceutical development of radiolabelled peptides. *Eur J Nucl Med Mol Imaging*. 2012;39:11-30.
16. Sauter AW, Mansi R, Hassiepen U, et al. Targeting of the cholecystokinin-2 receptor with the minigastrin analog ^{177}Lu-DOTA-PP-F11N: Does the use of protease inhibitors further improve in vivo distribution? *J Nucl Med*. 2019;60:393-399.
17. Klingler M, Summer D, Rangger C, et al. DOTA-MGS5, a new cholecystokinin-2 receptor-targeting peptide analog with an optimized targeting profile for theranostic use. *J Nucl Med*. 2019;60:1010-1016.
18. Zaknun JJ, Bodei L, Mueller-Brand J, et al. The joint IAEA, EANM, and SNMMI practical guidance on peptide receptor radionuclide therapy (PRRNT) in neuroendocrine tumours. *Eur J Nucl Med Mol Imaging*. 2013;40:800-816.
19. Vija A, Cachovan M. Automated internal dosimetry research tool using quantitative SPECT for the Lu177 theranostic application. *J Nucl Med*. 2017;58 (suppl 1):1301.
20. Hindorf C, Glatting G, Chiesa C, et al. EANM Dosimetry Committee guidelines for bone marrow and whole-body dosimetry. *Eur J Nucl Med Mol Imaging*. 2010;37:1238-1250.

Downloaded from jnm.snmjournals.org by Universitaetsbibliothek Bern on January 8, 2020. For personal use only.

21. Bozkurt MF, Virgolini I, Balogova S, et al. Guideline for PET/CT imaging of neuroendocrine neoplasms with ^{68}Ga-DOTA-conjugated somatostatin receptor targeting peptides and ^{18}F-DOPA. *Eur J Nucl Med Mol Imaging*. 2017;44:1588-1601.
22. Wild D, Fani M, Fischer R, et al. Comparison of somatostatin receptor agonist and antagonist for peptide receptor radionuclide therapy: a pilot study. *J Nucl Med*. 2014;55:1248-1252.
23. Reubi JC, Chayvialle JA, Franc B, et al. Somatostatin receptors and somatostatin content in medullary thyroid carcinomas. *Lab Invest*. 1991;64:567-573.
24. Emami B, Lyman J, Brown A, et al. Tolerance of normal tissue to therapeutic irradiation. *Int J Radiat Oncol Biol Phys*. 1991;21:109-122.
25. Barrett TD, Lagaud G, Wagaman P, et al. The cholecystokinin CCK2receptor antagonist, JNJ-26070109, inhibits gastric acid secretion and prevents omeprazole-induced acid rebound in the rat. *Br J Pharmacol*. 2012;166:1684–1693.

Downloaded from jnm.snmjournals.org by Universitaetsbibliothek Bern on January 8, 2020. For personal use only.

FIGURES

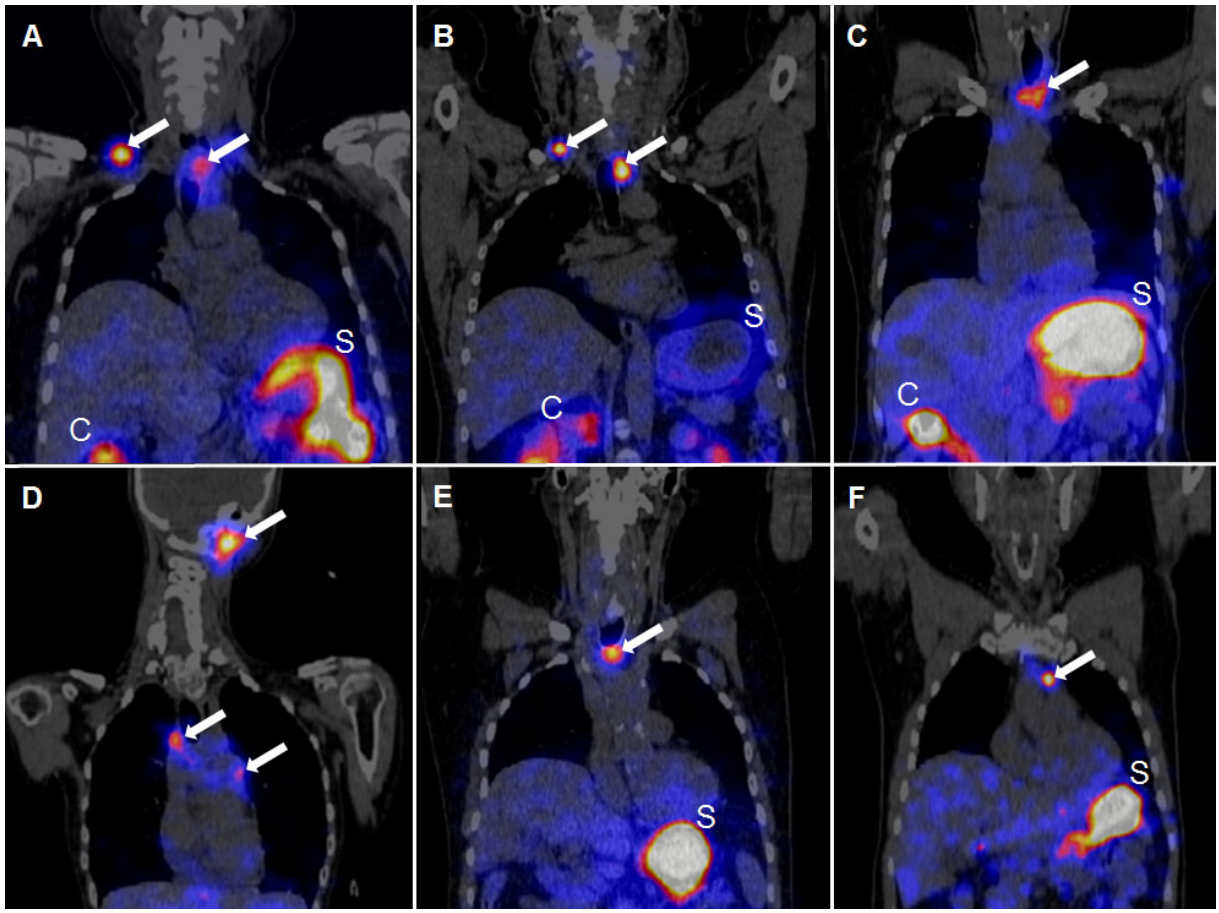

FIGURE 1. ^{177}Lu-PP-F11N SPECT/CT scans 24 h p.i. in coronar orientation. In all 6 patients (A-F: patient 1-6), several tumors were visualized with SPECT (white arrows). Minimal diameter of a detectable tumor was 8 mm (F: patient 6). S = stomach, C = colon.

Downloaded from jnm.snmjournals.org by Universitaetsbibliothek Bern on January 8, 2020. For personal use only.

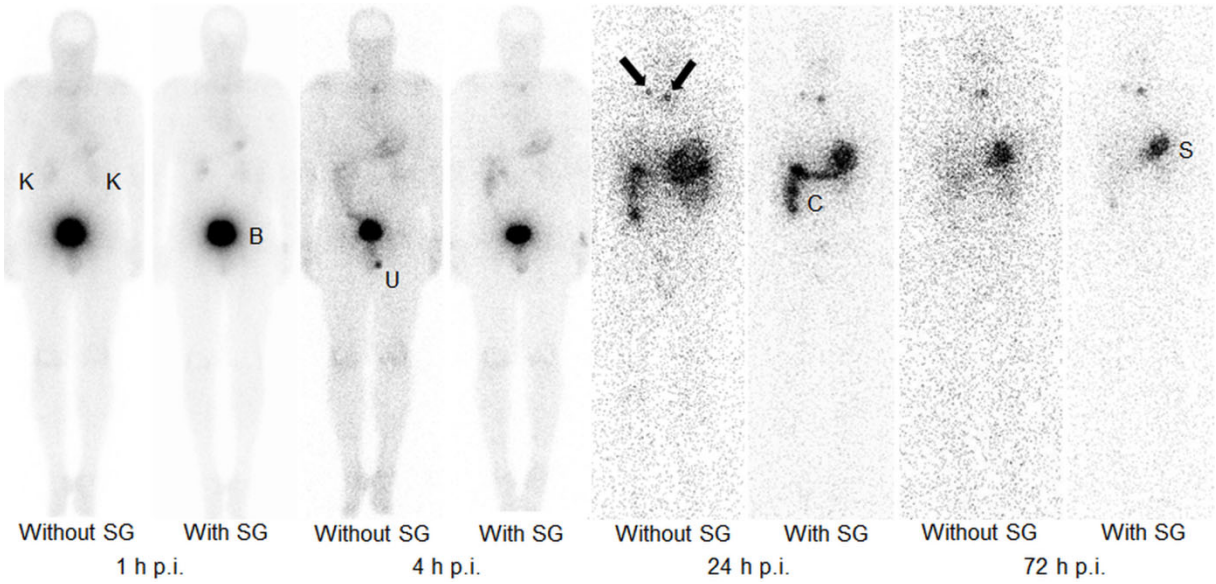

FIGURE 2. Planar scans (anterior view) of patient 2 without and with co-administration of succinylated gelatin (SG) at 1, 4, 24 and 72 h after injection of 1 GBq of ^{177}Lu-PP-F11N. On planar scans two tumors with a diameter of 10 x 10 mm and 7 x 18 mm (black arrows) were visible. K: kidneys, C: colon, S: stomach, B: urinary bladder, U: urine contamination.

Downloaded from jnm.snmjournals.org by Universitaetsbibliothek Bern on January 8, 2020. For personal use only.

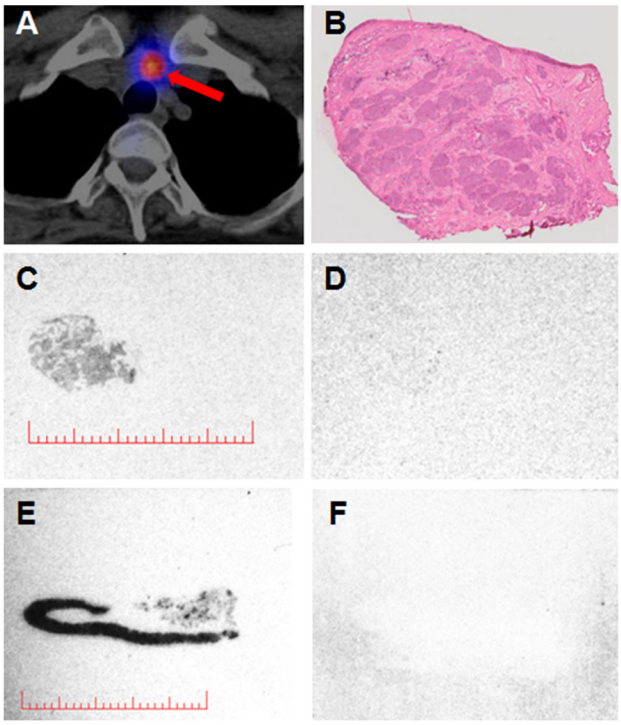

FIGURE 3. Images from patient 3, showing the axial ^{177}Lu-PP-F11N SPECT/CT scan (A) of a suspicious lymph node (red arrow) with the corresponding hematoxylin-eosin-stained tissue (B) and *in vitro* autoradiograms of adjacent sections indicating total binding of ^{111}In-PP-F11N (C) and non-specific binding (D). E and F show dog stomach tissue as a positive control. An 9 x 9 mm lesion with uptake in SPECT/CT (A) corresponds to a lymph node metastasis with 60% tumor cells (B) and specific ^{111}In-PP-F11N binding (C and D). Red bars: 10 mm. See Supplemental Fig. 1 for additional series.

TABLE 1. Absorbed radiation doses of ^{177}Lu-PP-F11N in tumors, kidneys, stomach and bone marrow without and with co-administration of succinylated gelatin.

*Test for superiority: two-sample paired sign test with a significance level, α, of 0.05. Abbreviation: SG = succinylated gelatin

Patient	Mean tumor dose (Gy/GBq) per patient		Mean kidney dose (Gy/GBq) per patient		Stomach dose (Gy/GBq)		Bone marrow dose (Gy/GBq)		Tumor-to-kidney dose ratio		Tumor-to-stomach dose ratio		Tumor-to-bone marrow dose ratio	
SG	**Without**	**With**	**Without**	**With**	**Without**	**With**	**Without**	**With**	**Without**	**With**	**Without**	**With**	**Without**	**With**
1	1.09	1.04	0.15	0.11	0.45	0.50	0.022	0.025	7.27	9.45	2.42	2.08	49.6	41.6
2	3.59	1.42	0.13	0.07	0.38	0.47	0.025	0.028	27.6	20.3	9.45	3.02	143.6	50.7
3	0.90	0.67	0.06	0.05	1.66	1.46	0.028	0.031	15	13.4	0.54	0.46	32.1	21.6
4	0.85	0.64	0.08	0.10	0.20	0.18	0.044	0.039	10.6	6.4	4.25	3.56	19.3	16.4
5	0.85	1.03	0.13	0.05	1.2	2.07	0.036	0.039	6.5	20.6	0.71	0.50	23.6	26.4
6	0.63	0.63	0.05	0.05	0.13	0.26	0.028	0.033	12.6	12.6	4.85	2.42	22.5	19.1
Median	0.88	0.85	0.11	0.06	0.42	0.49	0.028	0.032	11.6	13	3.34	2.25	27.9	24
IQR	0.85-1.04	0.65-1.04	0.07-0.13	0.05-0.09	0.25-1.01	0.31-1.22	0.026-0.034	0.025-0.038	8.11-14.4	10.2-18.6	1.14-4.70	0.90-2.87	19.3-45.2	16.4-37.8
Test for superiority*	*P* = 0.38		*P* = 0.38		*P* = 0.69		*P* = 0.22		*P* = 1.0		*P* = 0.16		*P* = 0.22	

Downloaded from jnm.snmjournals.org by Universitaetsbibliothek Bern on January 8, 2020. For personal use only.

Downloaded from jnm.snmjournals.org by Universitaetsbibliothek Bern on January 8, 2020. For personal use only.

TABLE 2. Adverse events (AE) observed following injection of ^{177}Lu-PP-F11N

Patient No.	AE without SG	AE with SG	Intensity*	Relationship
1	Hot flushes	Hot flushes	Grade 1	Probable
2	Hot flushes	Hot flushes	Grade 1	Probable
	Nausea and vomiting	Nausea and vomiting	Grade 1	Probable
	Paresthesia	Paresthesia	Grade 1	Probable
	Toothache	Toothache	Grade 1	Probable
		Hypotension	Grade 1	Probable
	Fatigue		Grade 1	Possible
	Headache		Grade 1	Possible
3	Numbness		Grade 1	Probable
	Hypotension	Hypotension	Grade 1	Probable
4	Nausea and vomiting	Nausea and vomiting	Grade 1	Probable
	Tachycardia		Grade 1	Probable
		Hypotension	Grade 1	Possible
	Hypocalcemia		Grade 1	Possible
		Fatigue	Grade 1	Probable
		Hypokalemia	Grade 1	Probable
5		Hot flushes	Grade 1	Probable
	Hypocalcemia	Hypocalcemia	Grade 1	Probable
		Hypokalemia	Grade 1	Possible
	Nausea	Nausea	Grade 1	Probable
		Dizziness	Grade 1	Probable
	Abdominal pain		Grade 1	Possible
6	Hypotension	Hypotension	Grade 1	Probable
	Hypokalemia		Grade 1	Possible

*Graded according to CTCAE (Common Terminology Criteria for Adverse Events) version 4.03.

Abbreviation: SG = succinylated gelatin

Downloaded from jnm.snmjournals.org by Universitaetsbibliothek Bern on January 8, 2020. For personal use only.

Supplemental Data

Cholecystokinin-2 Receptor Agonist 177Lu-PP-F11N for Radionuclide Therapy of Medullary Thyroid Carcinoma - Results of the Lumed Phase 0a Study

Dosimetry

2D dosimetry was performed for the bladder (all patients) and large intestine, if visible at more than one time point on images, which was the case in one patient. For all imaging time points, regions of interest were manually drawn around the whole body, bladder and, if applicable, large intestine, on both the anterior and the posterior scans. Background regions were placed close to the regions of interest for background correction. The geometric mean value, between anterior and posterior, was taken and corrected for attenuation using the conjugate-view method. Whole-body activity acquired at 1 hour after injection of ^{177}Lu-PP-F11N was set as 100 percentage injected activity. Time-activity curves derived from the whole-body studies were analyzed with the OLINDA/EXAM 1.0 (Vanderbilt University, TN, USA) software. Organ doses were calculated with the OLINDA/EXAM 1.0 whole-body female and male phantom. For this calculation stomach and kidney numbers of disintegrations for the source organs were obtained from 3D dosimetry data. In doing so the gamma radiation cross-fire effect from stomach and kidneys to the other organs is considered. Blood marrow doses were determined by the blood-based red marrow dose methodology, which assumes a linear relation between the blood residence time and the red marrow residence time. For dosimetry calculations with OLINDA/EXAM 1.0 a blood-to-red-marrow activity concentration radio of 1 was used as recommended by the European Association of Nuclear Medicine. Final organ dosimetry results which are presented in Supplemental Table 2 are based on OLINDA/EXAM 1.0 calculations except stomach and kidneys which were done with 3D volume-based MIRD dosimetry as described in the Method part of the manuscript.

Downloaded from jnm.snmjournals.org by Universitaetsbibliothek Bern on January 8, 2020. For personal use only.

Supplementary Table 1. Patients' demography and MTC characteristics

Patient no.	Age (y)	Sex	TNM	Time after first diagnosis (months)	Ct* before study enrollment (pg/ml)	CEA* before study enrollment (µg/l)
1	60	F	pT4 N1 Mx	129	3150	15.5
2	40	M	pT3 N1b M1	7	5900	64.8
3	54	F	pT4 N1 M0	186	1272	24.5
4	32	F	Tx N1 M1	125	53694	1436
5	67	M	Tx N1 Mx	230	226	3.3
6	46	M	pT3 N1b	8	134	2.7

*Abbreviations and normal laboratory values: Ct = calcitonin, normal value Ct < 8.6 pg/ml, CEA = carcinoembryonic antigen, normal value CEA < 3.4 µg/l

Downloaded from jnm.snmjournals.org by Universitaetsbibliothek Bern on January 8, 2020. For personal use only.

Supplementary Table 2. Absorbed organ and effective doses of ^{177}Lu-PP-F11N without and with co-administration of succinylated gelatin.

Organ/tissue	Median absorbed radiation dose in Gy/GBq (IQR)		Test for superiority*
	Without SG	With SG	*P* =
Adrenals	0.0012 (0.0008-0.0021)	0.0011 (0.0008-0.0024)	1.00
Brain	0.0000	0.0000	1.00
Breasts	0.0002 (0.0001-0.0004)	0.0002 (0.0001-0.0005)	0.22
Gallbladder wall	0.0011 (0.0008-0.0021)	0.0012 (0.0007-0.0029)	1.00
LLI wall	0.0017 (0.0009-0.0025)	0.0011 (0.0010-0.0016)	0.38
Small intestine	0.0013 (0.0009-0.0016)	0.0010 (0.0007-0.0021)	0.69
Stomach wall	0.42 (0.25-1.01)	0.49 (0.31-1.22)	0.69
ULI wall	0.0012 (0.0010-0.0019)	0.0011 (0.0008-0.0025)	1
Heart wall	0.0007 (0.0005-0.0015)	0.0080 (0.0005-0.0021)	0.69
Kidneys	0.11 (0.067-0.13)	0.062 (0.053-0.093)	0.38
Liver	0.0006 (0.0004-0.0011)	0.0006 (0.0004-0.0015)	0.69
Lungs	0.0004 (0.0003-0.0007)	0.0004 (0.0003-0.0011)	0.03
Muscle	0.0007 (0.0005-0.0009)	0.0005 (0.0004-0.0011)	0.69
Ovaries	0.0012 (0.0008-0.0017)	0.0010 (0.0009-0.0013)	0.69
Pancreas	0.0035 (0.0022-0.0079)	0.0039 (0.0025-0.0010)	0.69
Red marrow	0.0280 (0.026-0.034)	0.0320 (0.025-0.0375)	0.22
Osteogenic cells	0.0066 (0.0053-0.0082)	0.0074 (0.0062-0.0088)	0.22
Skin	0.0002 (0.0002-0.0003)	0.0002 (0.0001-0.0004)	0.13
Spleen	0.0023 (0.0014-0.0051)	0.0025 (0.0016-0.0058)	0.69
Testes	0.0002 (0.0-0.0004)	0.0002 (0.0-0.0004)	0.25
Thymus	0.0001 (0.0001-0.0003)	0.0001 (0.0001-0.0004)	0.30
Thyroid	Not applicable †	Not applicable †	
Urinary bladder wall	0.27 (0.22-0.37)	0.26 (0.23-0.32)	0.69
Uterus	0.0018 (0.0015-0.0027)	0.0018 (0.0017-0.0020)	0.69
Total body	0.0030 (0.0023-0.0041)	0.0025 (0.0021-0.0050)	0.69
Effective dose (Sv/GBq)	0.077 (0.062-0.138)	0.075 (0.051-0.167)	0.69

*Test for superiority: two-sample paired sign test with a significance level, α, of 0.05. † Not applicable as all patients had previous thyroidectomy. Abbreviation: SG = succinylated gelatin, LLI = lower large intestine; ULI = upper large intestine

Downloaded from jnm.snmjournals.org by Universitaetsbibliothek Bern on January 8, 2020. For personal use only.

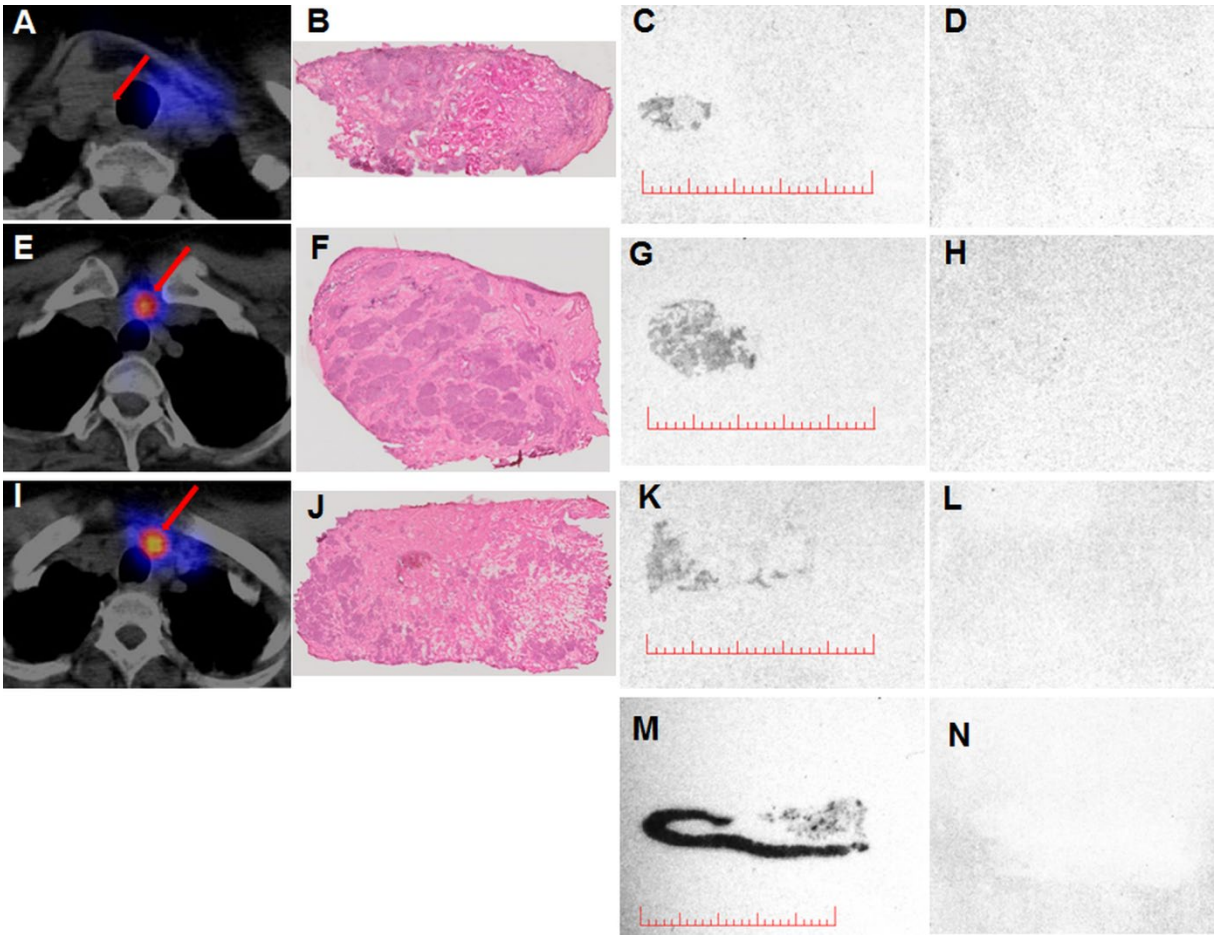

Supplementary Figure 1. Images from patient 3 showing axial ^{177}Lu-PP-F11N SPECT/CT scans (A,E,I) of suspicious lymph nodes (red arrows), with corresponding histology and *in vitro* autoradiography results in the same row: fraction of hematoxylin-eosin-stained sections (B,F,J) together with autoradiograms indicating total binding of ^{111}In-PP-F11N (C,G,K) and non-specific binding (D,H,L). M and N show dog stomach tissue as a positive control. First row: 8 x 8 mm lesion without uptake in SPECT/CT (A, red arrow) corresponds to a lymph node metastasis with 40% tumor cells (B) with specific ^{111}In-PP-F11N binding (C and D). Second row: 9 x 9 mm lesion with uptake in SPECT/CT (E, red arrow) corresponds to a lymph node metastasis with 60% tumor cells (F) with specific ^{111}In-PP-F11N binding (G and H). Third row: 16 x 18 mm lesion with uptake in SPECT/CT (I, red arrow) corresponds to a lymph node metastasis with 40% tumor cells (J) with specific ^{111}In-PP-F11N binding (K and L). Red bars: 10 mm.

Downloaded from jnm.snmjournals.org by Universitaetsbibliothek Bern on January 8, 2020. For personal use only.

The Journal of NUCLEAR MEDICINE

Cholecystokinin-2 Receptor Agonist ^{177}Lu-PP-F11N for Radionuclide Therapy of Medullary Thyroid Carcinoma - Results of the Lumed Phase 0a Study

Christof Rottenburger, Guillaume P Nicolas, Lisa McDougall, Felix Kaul, Michal Cachovan, A Hans Vija, Roger Schibli, Susanne Geistlich, Anne Schumann, Tilman Rau, Kathrin Glatz, Martin Behe, Emanuel R. Christ and Damian Wild

J Nucl Med.
Published online: September 13, 2019.
Doi: 10.2967/jnumed.119.233031

This article and updated information are available at:
http://jnm.snmjournals.org/content/early/2019/09/19/jnumed.119.233031

Information about reproducing figures, tables, or other portions of this article can be found online at:
http://jnm.snmjournals.org/site/misc/permission.xhtml

Information about subscriptions to JNM can be found at:
http://jnm.snmjournals.org/site/subscriptions/online.xhtml

JNM ahead of print articles have been peer reviewed and accepted for publication in *JNM*. They have not been copyedited, nor have they appeared in a print or online issue of the journal. Once the accepted manuscripts appear in the *JNM* ahead of print area, they will be prepared for print and online publication, which includes copyediting, typesetting, proofreading, and author review. This process may lead to differences between the accepted version of the manuscript and the final, published version.

The Journal of Nuclear Medicine is published monthly.
SNMMI | Society of Nuclear Medicine and Molecular Imaging
1850 Samuel Morse Drive, Reston, VA 20190.
(Print ISSN: 0161-5505, Online ISSN: 2159-662X)

© Copyright 2019 SNMMI; all rights reserved.

SNMMI SOCIETY OF NUCLEAR MEDICINE AND MOLECULAR IMAGING